

**RADIOCHEMISTRY  
AND RADIOPHARMACEUTICALS**

**[<sup>18</sup>F]-Labeled 3-Deoxy-3-Fluoro-D-Glucose:  
Synthesis and Preliminary  
Blodistribution Data**

Timothy J. Tewson, Michael J. Welch, and Marcus E. Raichle

*Mallinckrodt Institute of Radiology, St. Louis, Missouri*

*A cyclotron target system for the production of anhydrous [<sup>18</sup>F] fluoride ion has been developed and used for the synthesis of carrier-free [<sup>18</sup>F]-3-deoxy-3-fluoro-D-glucose (3-FDG). The synthesis is sufficiently rapid and efficient to allow production of usable amounts of 3-FDG with a 6-MeV cyclotron. Preliminary animal studies show that 3-FDG is in fact a glucose analog.*

**J Nucl Med 19: 1339-1345, 1978**

The development of positron-emission tomography, coupled with the synthesis of biologic substrates containing positron-emitting nuclides, makes it possible to study local metabolism in vivo by noninvasive techniques. Carbon-11-labeled glucose has been used to determine local glucose metabolism in the brain (1), but the rapid metabolic turnover leads to the egress of <sup>11</sup>CO<sub>2</sub>. A glucose analog that would be transported like glucose and enter but not complete the metabolic cycle would be desirable. The synthesis of such a compound has recently been published, [<sup>18</sup>F]-2-deoxy-2-fluoro-D-glucose (2-FDG) (2). It is available only with a large cyclotron.

Of the possible isomers of deoxy-fluoro-glucose, the 6-fluoro cannot be phosphorylated at C-6, the 5-fluoro prevents the formation of the pyranose ring, and the 4-fluoro rapidly loses fluoride ion in vivo (3), as do the alpha and beta glucosyl fluorides with fluorination at C-1 (4).

Controlled transport across cell membranes involves either "active transport" or "facilitated diffusion" (5). Both processes involve a carrier and have a significant activation energy (10-12 kcal/

mole). For a given concentration gradient, facilitated diffusion is considerably faster than would be expected from a passive mechanism. Active transport is an energy-consuming process, moving the substrate against a concentration gradient. The in vitro studies of these two transport systems have been performed on the hamster intestine for active transport (6) and on the human erythrocyte for facilitated diffusion (7). The blood-brain barrier is extremely difficult to study in vitro. There is, however, considerable in vivo evidence, both direct and indirect, that transport of glucose across the blood-brain barrier is similar to that in the human erythrocyte—that is, a facilitated diffusion. Both systems are sodium-independent, are insensitive to insulin, and respond like transport inhibitors such as phloretin, phlorizin, and cytochalasin B (8). Both systems also respond in a similar quantitative fashion to a variety

Received March 22, 1978; revision accepted July 5, 1978.

For reprints contact: T. J. Tewson, Div. of Radiation Sciences, Mallinckrodt Institute of Radiology, 510 South Kingshighway, St. Louis, MO 63110.

of glucose analogs (8), although the blood-brain barrier and the erythrocyte membrane show differing selectivities for the alpha and beta anomers of glucose.

Because the brain is not the only organ of interest with respect to glucose metabolism, a glucose analog that fulfills the requirements for both active transport and facilitated diffusion is obviously desirable. In vitro studies (9) using the hamster's small intestine (active transport model) show that an alpha-hydroxyl group is required at C-2, possibly for the formation of a covalent bond, while a hydrogen bond acceptor is required at C-3 (9), and this is possible when a fluorine is substituted for the 3- $\beta$ -hydroxyl. Thus, 2-deoxy-2-fluoro-D-glucose is not actively transported and 3-deoxy-D-glucose is transported poorly, while 3-deoxy-fluoroglucose is transported with  $K_i$  and  $V_{max}$  similar to those of glucose (9).

For the human erythrocyte model (facilitated diffusion), no one hydroxyl group is essential for transport. 3-Deoxy-3-fluoro-D-glucose is transported with constants very similar to those obtained for glucose (10,11). Data are not available for 2-FDG, but it is possible that the two position is not involved with binding to this carrier (10,11).

The first metabolic step, which is essential to prevent the glucose analog from leaving the cell as rapidly as it arrived, is phosphorylation at the six position. Studies with yeast hexokinase have shown that 2-FDG is a good substrate, while 3-FDG is phosphorylated with rates only ~5–10% of those for glucose (12). 2-FDG has been shown to inhibit totally the hexokinase in ascites tumor cells (13), while 3-FDG is a good substrate for the phosphoenolpyruvate-dependent phosphotransferase and hexokinase systems in *E. coli* and yeast (14,15). With material of very high specific activity, however, when enzyme/substrate ratios are very high and the reaction is irreversible, the actual substrate/enzyme affinities are probably less important than for the conventional system when enzyme/substrate ratios are very low. At this time the relationship of the enzymes studied to the actual phosphorylating enzymes in the brain is not clear.

The metabolic fate of 3-FDG has been shown to be species-dependent, but the tissue accumulates either 3-deoxy-3-fluoro-D-glucitol or further oxidation products that still contain fluorine (16,17).

Finally, 3-FDG has been shown to be nontoxic in rats at doses of 5 g/kg (17). Thus it appears to be an attractive candidate for synthesis with F-18 and use as a metabolic analog with a positron-imaging device.

Standard methods for the synthesis of 3-FDG

(18) require 6 days for the complete reaction sequence, and thus are not suitable for use with F-18 ( $T_{1/2} = 110$  min). We have developed a rapid synthetic sequence (Fig. 1) that is amenable to use with cyclotron-produced radionuclides (19). It is based upon fluoride ion displacement of 1,2:5,6-di-O-isopropylidene- $\alpha$ -D-allofuranose (IV). II, III, and IV were all prepared according to published procedures (20,21), and 1,2:5,6-di-O-isopropylidene-3-deoxy-3-fluoro- $\alpha$ -D-glucofuranose (V) was identified by comparison of NMR, IR, and mass spectra with published data (22). 3-FDG (VI), obtained by boron trichloride hydrolysis of the di-isopropylidene groups, has not been obtained as crystals, but is chromatographically identical\* with that obtained from conventional acid hydrolysis (18). Moreover, the tetra-acetates (VII) obtained from either route are identical (M.Pt. mixed M.Pt.) (18).

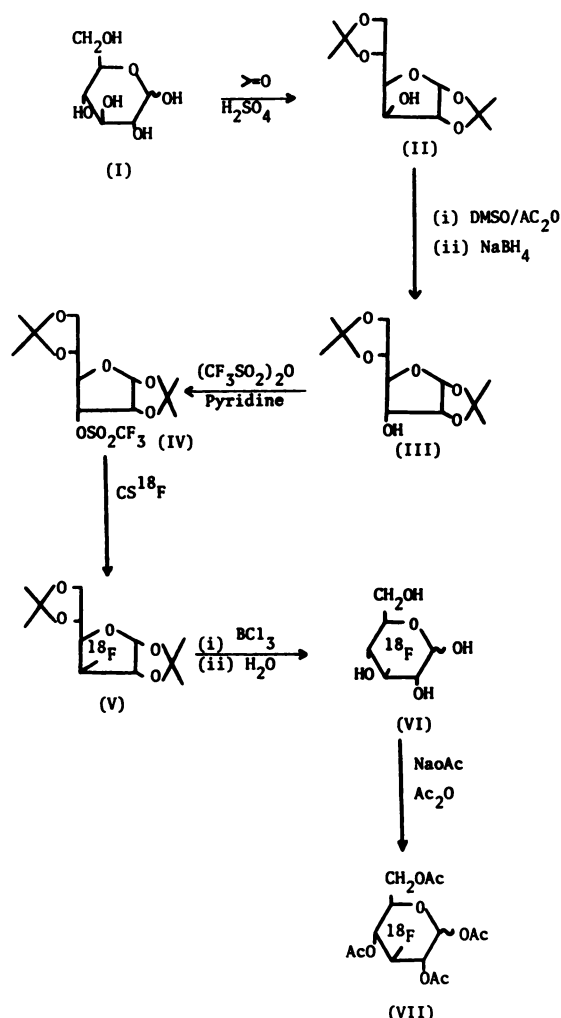
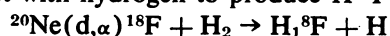


FIG. 1. Synthetic sequence for synthesis of 3-FDG (VI).

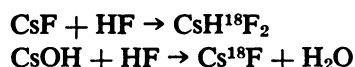
[<sup>18</sup>F] fluoride ion is commonly produced by bombardment of water with a variety of particles (23). However, fluoride ion has a tightly bound solvation sphere that considerably reduces its nucleophilicity and is also very difficult to remove (24). Therefore a target system was developed that would allow the production of anhydrous [<sup>18</sup>F] fluoride ion.

#### MATERIALS AND METHODS

**Cyclotron system.** The target for production of H<sup>18</sup>F has been described previously (25). Neon containing 15% H<sub>2</sub> is bombarded with 5.2-MeV deuterons (on target) to produce F-18 atoms, which then react with hydrogen to produce H<sup>18</sup>F:



The gases are circulated rapidly during bombardment by a peristaltic pump and pass over either a glass-wool plug coated with cesium fluoride or a silver-wool plug coated with cesium hydroxide. These absorb the H<sup>18</sup>F:



No measurable activity passes the glass-wool plug, and >60%† of the produced activity is removed from the target chamber. A 10 μAhr bombardment produces 16–18 mCi adsorbed on the glass wool. The silver-wool/cesium-hydroxide is less successful at trapping the activity, probably because the silver wool is much coarser than the glass and the cesium hydroxide adheres less and is thus more easily knocked off. A 10 μAhr bombardment produces 12–13 mCi adsorbed on the wool. The remainder passes through and accumulates in the plastic loop of the pump.

**Synthetic procedures and analysis.** *Carrier procedure.* The glass-wool plug containing the activity was added to a solution of 25 mg of (IV) (19) and 5 mg N,N,N',N'-tetramethyl-1,8-diaminonaphthalene (proton sponge) in dimethylformamide (2 ml, freshly distilled from calcium hydride under reduced pressure) and refluxed for 45 min. Injection of this solution onto a radiogaschromatograph (6' OV-1 column, 180°C, flow rate 30 ml/min) revealed that approximately 98% of the volatile activity, and 70% of the activity in solution, are incorporated into (V). Addition of authentic (V) to the solution has no effect on the activity peak. However, this incorporation is anomalously high, probably due to further reaction on the chromatographic injection block. TLC analysis (silica plates, 1% MeOH/CH<sub>2</sub>Cl<sub>2</sub>) of the product of the reaction shows that ~50% of the activity remains at the origin and ~50% has an R<sub>f</sub> of 0.6 [R<sub>f</sub> of (V) = 0.6]. One to two percent of the

activity is in the band R<sub>f</sub> = 0.9, where the trifluoromethane sulfonate IV appears. The solution is then poured into ether (25 ml) and the glass wool washed twice with 2-ml portions of ether, dried with magnesium sulfate, and evaporated to dryness. The residue is dissolved in methylene chloride (3 ml), 2 M in boron trichloride, allowed to stand for 5 min, and 2 ml water added. The methylene chloride is evaporated, the solution neutralized with sodium hydroxide, and purified on an ion-exchange column. The solution is then evaporated down to 2 ml, neutralized with NaOH, and filtered through a Millipore filter. A small sample is injected onto a Waters carbohydrate column, eluted with 85% CH<sub>3</sub>CN/H<sub>2</sub>O (2 ml/min), resulting in a single radioactive peak at 6 min, identical with that from an authentic sample of VI. A typical run produces 2–2.5 mCi of injectable activity from a 35 μA-hr bombardment (55 mCi), with a minimum specific activity of 50 mCi per millimol at 90 min from EOB.

*Carrier-free procedure.* The failure to wash all the activity from the glass wool was obviously unsatisfactory. Also an increase in the specific activity was desirable. Accordingly, the silver-wool/cesium-hydroxide trapping system was used. The silver-wool/cesium-hydroxide plug containing the activity is added to a solution of IV (25 mg) and proton sponge (5 mg) in hexamethyl phosphoric triamide (HMPA) (2 ml) freshly distilled under vacuum from 13× molecular sieves; the solution is then heated to 150°C in an oil bath for 1 hr while nitrogen is bubbled slowly through the solution. It is allowed to cool and then poured into ether (25 ml), and the flask and silver wool are washed twice with ether (2 × 5 ml). Less than 10% of the activity remains in the flask and on the silver wool.

The ether is washed with water (3 × 25 ml), which typically also washes less than 10% of the activity from the ether layer. GC analysis of this solution with our present system has been unsuccessful with carrier-free V. The very small amount of material appears to be nonselectively adsorbed, and tailing of the peak makes it virtually undetectable. However, this analysis does establish that all the HMPA is washed from the ether solution. TLC analysis (silica-gel plates, 2% MeOH/CH<sub>2</sub>Cl<sub>2</sub>) shows that virtually all the activity runs with the same R<sub>f</sub> as V.

The ethereal solution is then treated in the same fashion as the carrier-containing material. The final result from a 10 μAhr bombardment (12–13 mCi adsorbed activity) is 4.5–5 mCi of [<sup>18</sup>F]-3-FDG at the end of synthesis ready for injection. If the [<sup>18</sup>F]-3-FDG is carrier free (see Discussion) it has a

specific activity of  $1.2 \times 10^4$  Ci/mg. The difference in yield between the carrier and carrier-free procedures is almost certainly due to the different fluorine species present on the glass wool (*vide infra*). In one experiment performed, using carrier fluoride but the carrier-free procedure—i.e., silver wool and HMPA—the radiochemical yield was the same as for the carrier-free procedure.

**Animal studies.** The blood-brain barrier permeability to 3-FDG was assessed in rhesus monkeys (*Macaca mulatta*) by external detection of a small bolus ( $\sim 0.2$  ml) of the tracer injected into the internal carotid artery. This measurement was complemented by the simultaneous measurement of cerebral blood flow (CBF) and cerebral metabolic rate for glucose, determined respectively from the external detection of the washout of  $H_2^{15}O$  injected into the internal carotid artery and the brain arteriovenous difference for plasma glucose concentration as measured by standard enzymatic techniques. The details of the experimental procedures have been described elsewhere (26). Briefly, to assure that the radionuclides entered only the internal carotid artery, the right external carotid artery was ligated at the bifurcation of the common carotid artery 2 wk before the experiment. This surgical procedure facilitates the injection of tracers into the internal carotid artery, and its effect on our experimental results is considered negligible (26). For the experiment reported here, the monkeys were anesthetized with phencyclidine (Sernylan, 3 mg/kg), paralyzed with gallium triethiodide (Flaxidyl), intubated with a cuffed endotracheal tube, and passively ventilated with an animal respirator on 100% oxygen. A 1.4-mm catheter was inserted in the femoral artery and its tip positioned in the right common carotid artery under fluoroscopic guidance. A second catheter was positioned in the right jugular bulb for the collection of cerebral venous blood, and a second injection of [ $^{18}F$ ]-3-FDG used in the correction of our arterial injection for recirculating tracer (see below). To prevent clotting in these catheter systems, the animal was given heparin at the beginning of the experiment. Routine monitoring of the animal included the continuous measurement of arterial blood pressure, end-tidal carbon dioxide tension, and rectal temperature.

The time course of labeled 3-FDG and O-15-labeled blood through the brain was detected by a NaI(Tl) detector (3 in.  $\times$  2 in.) appropriately positioned and collimated to insure uniform detection efficiency. After suitable electronic processing—including narrow pulse-height analysis—the signals were processed in a classic LINC laboratory computer, and corrections made for tracer decay and room background. Temporal resolution of the data

was optimized in the initial portion of each collection by using sample integration times of 0.1 sec.

The extraction fraction of labeled 3-FDG was obtained by graphically extrapolating the nearly linear 25–60 sec section of the semilogarithmic plot of tissue tracer clearance back to the abscissa of the maximum perfusion peak (Fig. 2), and computing the ratio of the extrapolated value to the value ob-

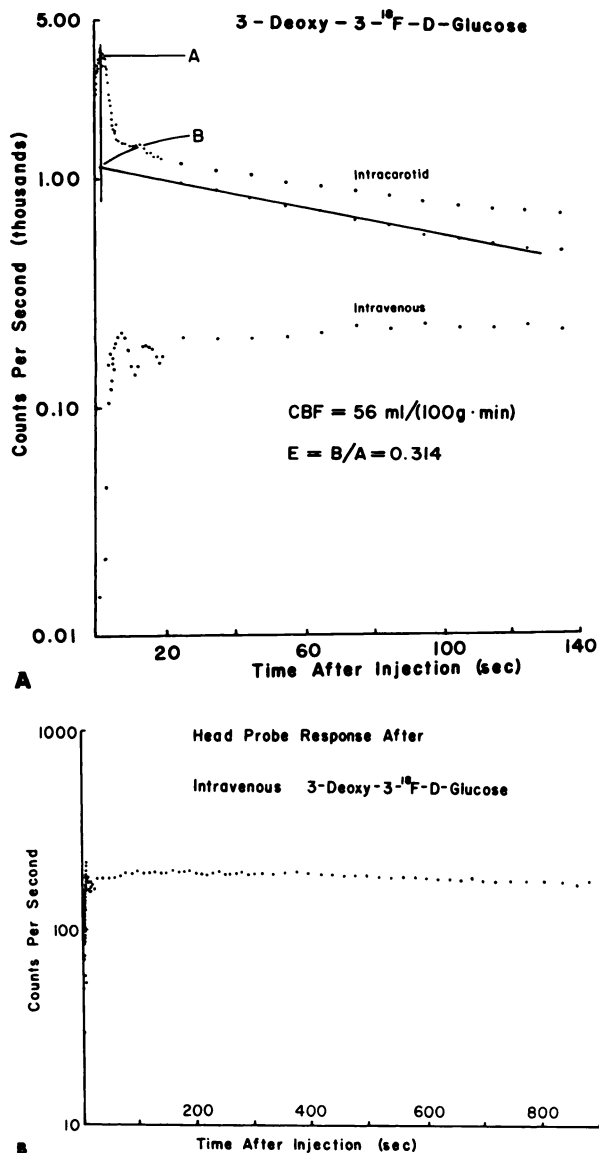


**FIG. 2.** (A) Behavior of [ $^{18}F$ ]-3-FDG during single capillary transit through the brain of rhesus monkey as seen by a single, externally placed scintillation detector (upper curve, "intracarotid"). The extraction (E) of [ $^{18}F$ ]-3-FDG by brain was computed from these data after correction was made for recirculating tracer by a second injection of tracer into venous effluent of brain (lower curve, "intravenous"), and "subtraction" of the two curves (see text). Extraction (E) was then computed from ratio of B to A as shown. Cerebral blood flow (CBF) was determined from clearance of  $H_2^{15}O$  following its carotid injection. (B) Behavior of [ $^{18}F$ ]-3-FDG in brain following its i.v. administration in rhesus monkey. Details of detection system are given in text.

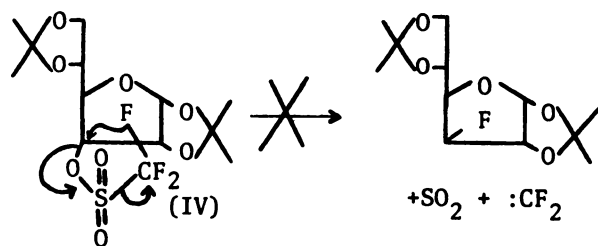


**FIG. 3.** Possible route for introduction of F-19 in synthesis of [<sup>18</sup>F]-3-FDG.

tained at A (Fig. 2). This initial estimate of the extraction fraction of [<sup>18</sup>F]-3-FDG is high because of the presence of significant recirculating tracer in the field of view of the detector. Correction for this recirculating tracer is made in the following manner. A second injection of labeled deoxyglucose is injected into the venous outflow of the brain by way of the catheter in the right jugular bulb. The quantity of tracer injected is normalized first to the amount injected into the carotid artery, and second to the first estimate of the nonextracted fraction as detailed above. The tracer curve generated from this injection (Fig. 2) is then used to subtract a first approximation of the amount of tracer present due to recirculation from the arterial tracer curve. From this corrected

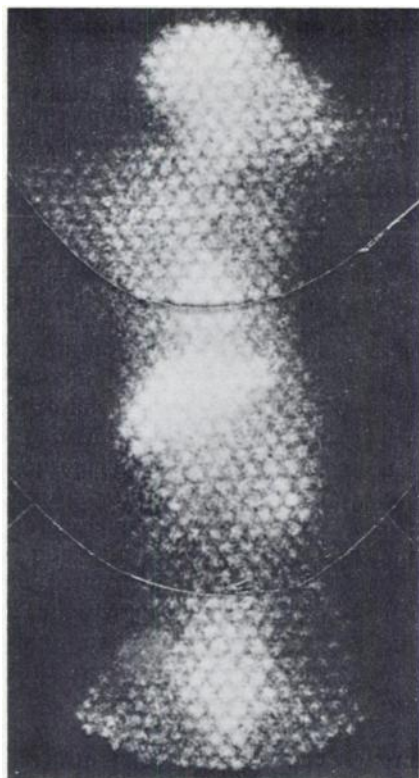


**FIG. 4.** Fluorine-18 distribution in rhesus monkey 30 minutes after injection of 6.5 mCi of [<sup>18</sup>F]-3-FDG.

arterial curve the venous data are renormalized and the subtraction procedure repeated. After three iterations of this procedure it can be shown (unpublished) that the true extraction fraction of a tracer such as 3-FDG can be determined from the arterial curve. The final extrapolated value (Fig. 2) is used to compute the actual fractional extraction of the tracer.

The cerebral metabolic rate for glucose was computed from the arteriovenous glucose difference and the CBF as measured by H<sub>2</sub><sup>15</sup>O.

In order to assess the behavior of [<sup>18</sup>F]-3-FDG in brain following its i.v. administration, 1 mCi was injected into a peripheral vein in an animal prepared and monitored in the manner described above.

Whole-body distribution data were obtained using a similarly anesthetized and paralyzed monkey, and injection of 6.5 mCi of [<sup>18</sup>F]-3-FDG. Scintigrams (200k counts/image) were obtained using a scintillation camera with a 550-keV-rated collimator, and the time taken for accumulation was recorded in each case. The results are shown in Fig. 4. The experiment was repeated with carrier-free material and the distribution was very similar.

#### RESULTS AND DISCUSSION

**Radiochemistry.** The reaction between cesium fluoride and the allose trifluoromethane sulfonate (IV) is close to quantitative with respect to both the ester and the fluorine ion (19), but with the radiotracer considerably less than 100% is incorporated. The primary variable is in the washoff from the glass wool plug. This is not surprising. Cesium fluoride is known to react with glass in the presence of water to produce fluorinated silicone derivatives, which can either be freed from the surface or remain in the polymeric structure of the glass. There is a rough correlation between the activity washed off the glass wool and that lost from the ether layer by the aqueous wash. Consequently the activity remaining in the ether layer is fairly constant, being 15% of the starting activity without correction for decay. This is consistent with increased removal of silicone fluorides rather than free fluoride ion. There is also the possibility of fluoride exchange with the trifluoromethane sulfonate anion. This occurs to a small extent with the ester (VI), and might occur to a larger extent with the anion produced by the displacement reaction.

Whether the silver-wool/cesium-hydroxide procedure truly produces carrier-free material or merely "no carrier added" is difficult to resolve fully. There are two possible sources of stable fluoride. The first is by thermal decomposition of the trifluoromethane sulfonate (IV) as shown in Fig. 3. This may oc-

cur on the injection block of the GC (250°C) when a small peak (1%) with a similar retention time as (V) is produced. It was determined by GC/MS that this was not (V). However, when (IV) is heated to 150°C in HMPA for 3 hr and then injected onto the GC, the chromatogram is identical to that produced by direct injection of (IV), and (IV) can be recovered quantitatively from the solution. Furthermore, if (IV) is refluxed in HMPA for 90 min (235°C), it is completely decomposed, but no detectable quantities of (V) are produced. Therefore it is unlikely, although not impossible, that small amounts of [<sup>19</sup>F] (V) are being produced by this route. Possibly stable fluorine is produced during the bombardment. Bombardment of the target produces micromolar quantities of methane by beam-induced decomposition of residual vacuum-pump oil and O-rings. The vacuum seals of the target are greased with "Fluorolube" high-vacuum grease, which is a polymeric fluorochloro-carbon. Irradiation of this grease in the reducing atmosphere could produce H<sup>19</sup>F, although the grease is out of the main radiation field and does not suffer any visible damage. Volatile fluorochlorocarbons could be expected to accompany the production of H<sup>19</sup>F, however, and none of these can be detected by IR or GC.

The available analytical techniques would indicate that no stable fluorine is being introduced, but the differences in sensitivity between what is detectable and what is truly "carrier free" are of the order of 10<sup>4</sup>.

**Animal experiments.** Behavior of [<sup>18</sup>F]-3-FDG during a single capillary transit through the brain is shown in Fig. 2. The CBF at the time of this measurement was 56 ml/(100 g min). The estimated extraction fraction (E) of [<sup>18</sup>F]-3-FDG, corrected for recirculating tracer, was 0.314. Arterial plasma glucose concentration was 93 mg%, and cerebral-venous plasma glucose concentration was 83 mg%. The computed cerebral metabolic rate for glucose was thus 5.6 mg/(100 g min).

These data (Fig. 2) suggest that [<sup>18</sup>F]-3-FDG crosses the blood-brain barrier by facilitated diffusion in a manner analogous to that of glucose (27). A preliminary estimate of the fidelity with which [<sup>18</sup>F]-3-FDG mimics the behavior of glucose can be obtained from our data. From the computed fractional extraction of [<sup>18</sup>F]-3-FDG we can estimate the forward flux of glucose across the blood-brain barrier. This is done by combining the arterial plasma glucose concentration, the fractional extraction of [<sup>18</sup>F]-3-FDG, and the computed CBF. This gives a value of 15.7 ml/(100 g min). From the ratio of the estimated forward flux to the net flux as computed

from the arteriovenous concentration difference for glucose and the CBF, we can estimate the ratio of glucose fluxes across the blood-brain barrier, as previously described (27). An estimate based on the tracer information provided by [<sup>18</sup>F]-3-FDG yields a value of 1.55. This is in good agreement with previous estimates of this value of 1.37 (27), and suggests, as described in detail elsewhere (27), that [<sup>18</sup>F]-3-FDG is faithfully mimicking the behavior of glucose during its passage across the blood-brain barrier. Further work will obviously be necessary to confirm this preliminary observation.

The behavior of [<sup>18</sup>F]-3-FDG in brain following its i.v. administration is shown in Fig. 2B. It is seen that [<sup>18</sup>F]-3-FDG activity rose promptly to a plateau value and remained relatively constant over the 900-sec period of data collection. These data demonstrate that [<sup>18</sup>F]-3-FDG is retained within brain tissue at a time when it can be estimated that blood activity has declined significantly, thus suggesting that this analog of glucose is trapped within the metabolic pathways of the brain as predicted. This observation, in conjunction with the blood-brain barrier permeability of [<sup>18</sup>F]-3-FDG as described above, lends preliminary support to the idea that this tracer may be useful in the measurement of glucose metabolism in the brain.

The whole-body distribution of carrier material as shown by the scintigrams (Fig. 4) is similar to that expected, since the brain, heart, and liver are the primary utilizers of glucose in the resting animal. The only anomaly is in the bladder. This is not unexpected, since in the rat 3-FDG accumulates in the bladder (17). The images were taken 5–70 min after injection, and no visual difference was seen over this time period. The difference in time taken to accumulate 200k counts over this time span is in the range of the half-life of F-18—i.e., for the head section 70 sec at 5 min and 95 sec at 70 min.

We have shown that, with a small cyclotron, usable quantities of very high-specific-activity [<sup>18</sup>F]-3-FDG can be synthesized. Note that the radiochemical yields obtained of [<sup>18</sup>F]-2-FDG are considerably less than those obtained in the current synthesis, and specific activities obtained with 3-FDG are higher than those obtained with 2-FDG (2).

#### FOOTNOTES

- \* Waters carbohydrate column, 85% acetonitrile/water.
- † Following irradiation of 100% neon, 3 mCi/μA-hr of F-18 can be washed out of the target chamber (M. J. Welch, unpublished data).

#### ACKNOWLEDGMENTS

This work was supported by U.S. PHS Grants 5 P01 HL13851 and 2 P50 NS0 6833.

We thank Steve Wittmer for preparing starting materials, Bill Margenau for preparing F-18, and Dr. M. M. Ter-Pogossian for his continued interest in this work.

#### REFERENCES

1. RAICHLER ME, WELCH MJ, GRUBB RL JR, et al: Measurement of regional substrate utilization rates by emission tomography. *Science* 199: 986-987, 1978
2. GALLAGHER BM, ANSARI A, ATKINS H, et al: Radiopharmaceuticals XXVII.  $^{18}\text{F}$ -labeled 2-deoxy-2-fluoro-D-glucose as a radiopharmaceutical for measuring regional myocardial glucose metabolism in vivo: Tissue distribution and imaging studies in animals. *J Nucl Med* 18: 990-996, 1977
3. TAYLOR NF, ROMASCHIN A, SMITH D: Metabolic and transport studies with deoxyfluoro monosaccharides. In *Biochemistry Involving Carbon-Fluorine Bonds*, Robert Fuller, ed. A.C.S. Symposium Series 28, Washington, D.C., American Chemical Society, 1976, pp 99-116
4. TAYLOR NF: The metabolism and enzymology of fluorocarbohydrates and related compounds. In *Carbon-Fluorine Compounds—A Ciba Symposium*. Amsterdam, Associated Scientific Publishers, 1972, pp 215-238
5. LEHNINGER AL: *Biochemistry*, 1st ed., New York, Worth Publishers, Inc., 1970, pp 605-627
6. BARNETT JEG, MONDAY KA: Structural requirements for active intestinal sugar transport in the hamster. In *Transport Across the Intestine—A Glaxo Symposium*. W. L. Burland, P. D. Samuel, eds. Baltimore, Williams and Wilkins Co., 1972, pp 111-127
7. BOLIS L, GOMPERS BD: Red blood cells. In *Transport and Accumulation in Biological Systems*. E. J. Harris, ed. London, Butterworth & Co., Ltd. Univ. Park Press, Baltimore), pp 93-146
8. BETZ AL, GILBOE DD, DREWES LR: The characteristics of glucose transport across the blood brain barrier and its relation to cerebral glucose metabolism. In *Transport Phenomena in the Nervous System: Physiological and Pathological Aspects*. In *Experimental Medicine and Biology*, vol. 69, G. Levi, L. Battistin, and A. Lajatha, eds. New York, Plenum Press, 1976, pp 133-149
9. BARNETT JEG: Fluorine as a substituent for oxygen in biological systems: Examples in mammalian membrane transport and glucosidase action. *Carbon-Fluorine Compounds Chemistry, Biochemistry and Biological Activities: A Ciba Foundation Symposium*. Amsterdam, Associated Scientific Publishers, 1972, pp 95-115
10. BARNETT JEG, HOLMAN GD, MONDAY KA: Structural requirements for binding to the sugar-transport system of the human erythrocyte. *Biochem J* 131: 211-221, 1973
11. RILEY GJ, TAYLOR NF: The interaction of 3-deoxy-3-fluoro-D-glucose with the hexose-transport system of the human erythrocyte. *Biochem J* 135: 773-777, 1973
12. BESSELL EM, FOSTER AB, WESTWOOD JH: The use of deoxyfluoro-D-gluco-pyranoses and related compounds in a study of yeast hexokinase specificity. *Biochem J* 128: 199-204, 1972
13. COE EL: Inhibition of glycolysis in Ascites tumor cells preincubated with 2-deoxy-2-fluoro-D-glucose. *Biochim Biophys Acta* 264: 319-327, 1972
14. WOODWARD B, TAYLOR NF, BRUNT RV: Effect of 3-deoxy-3-fluoro-D-glucose on glycolytic intermediates and adenine nucleotides in resting cells of *Saccharomyces cerevisiae*. *Biochem Pharmacol* 20: 1071-1077, 1971
15. MILES RJ, PIRT SJ: Inhibition by 3-deoxy-3-fluoro-D-glucose of utilization of lactose and other carbon sources by *Escherichia coli*. *J Gen Microbiol* 76: 305-318, 1973
16. TAYLOR NF, WHITE FH, EISENTHAL R: Oxidation of 3-deoxy-3-fluoro-D-glucose by cell-free extracts of *Pseudomonas fluorescens*. *Biochem Pharmacol* 21: 347-353, 1972
17. ROMASCHIN A, TAYLOR NF, SMITH DA, et al: The metabolism of 3-deoxy-3-fluoro-D-glucose by *Locusta migratoria* and *Schistocerca gregaria*. *Can J Biochem* 55: 369-375, 1977
18. FOSTER AB, HEMS R, WEBBER JM: Fluorinated carbohydrates. Part 1. 3-deoxy-3-fluoro-D-glucose. *Carbohydr Res* 5: 292-301, 1967
19. TEWSON TJ, WELCH MJ: New approaches to the synthesis of 3-deoxy-3-fluoroglucose. *J Org Chem* 43: 1090, 1978
20. STEVENS JD: Monosaccharides [16]  $\beta$ -D-Allose. In *Methods in Carbohydrate Chemistry*, vol 6, R. L. Whistler, J. N. BeMiller, eds. New York, Academic Press, 1972, pp 123-127
21. HALL LD, MILLER DC: Fluorinated sulphonic esters of sugars: Their synthesis and reactions with pyridine. *Carbohydr Res* 47: 299-305, 1976
22. FOSTER AB, HEMS R, HALL LD: Fluorinated carbohydrates. Part V. Nuclear magnetic resonance data on pyranose and furanose derivatives of 3-deoxy-3-fluoro-D-glucose. *Can J Chem* 48: 3937-3945, 1970
23. NOZAKI T, IWAMOTO M, IDO T: Yield of  $^{18}\text{F}$  for various reactions from oxygen and neon. *Int J Appl Radiation and Isotopes* 25: 393-399, 1974
24. CHAMBERS RD: *Fluorine in Organic Chemistry*. New York, John Wiley & Sons, 1973, p 21
25. STRAATMANN MG, WELCH MJ: Fluorine-18-labeled diethylaminosulfur trifluoride (DAST): An F-for-OH fluorinating agent. *J Nucl Med* 18: 151-158, 1977
26. RAICHLER ME, EICHLING JO, STRAATMANN MG, et al: Blood-brain barrier permeability of  $^{14}\text{C}$ -labeled alcohols and  $^{18}\text{O}$ -labeled water. *Am J Physiol* 230: 543-552, 1976
27. RAICHLER ME, LARSON KB, PHELPS ME, et al: In vivo measurement of brain glucose transport and metabolism employing glucose- $^{14}\text{C}$ . *Am J Physiol* 228: 1936-1948, 1975

#### BOOKS RECEIVED

*Health Implications of Nuclear Power Production*. Report on a Working Group, Brussels, December 1-5, 1975. 75 pp. Copenhagen, WHO Regional Office for Europe, 1978 (WHO Regional Publications, European Series No. 3: ISBN: 92 9020 103 7). Sw.fr. 8.-, US\$ 4.-  
*The Radiobiology of Human Cancer Radiotherapy*, 2nd ed., J. Robert Andrews. 591 pp, illustrated. Baltimore, University Park Press, 1978. \$39.50